IEEE Access
Multidisciplinary | Rapid Review | Open Access Journal

Received 28 November 2022, accepted 13 December 2022, date of publication 15 December 2022,
date of current version 22 December 2022.

Digital Object Identifier 10.1109/ACCESS.2022.3229698

RESEARCH ARTICLE

An Intelligent Deep Convolutional Neural Networks-Based Islanding Detection for Multi-DG Systems

ARIF HUSSAIN, (Member, IEEE), CHUL-HWAN KIM, (Fellow, IEEE), AND MUHAMMAD SHAHID JABBAR

Department of Electrical and Computer Engineering, Sungkyunkwan University, Suwon 16419, South Korea

Corresponding author: Chul-Hwan Kim (chkim@skku.edu)

This work was supported by the National Research Foundation of Korea (NRF) Grant through the Korean Government [Ministry of Science, ICT and Future Planning (MSIP)] under Grant 2021R1A2B5B03086257.

ABSTRACT Unintentional islanding is a problem in electrical distribution networks; it happens when the central utility is unintentionally separated from the rest of the distributed power system. The islanding detection problem becomes severe in non-detection zones. We propose an intelligent islanding detection technique with zero non-detection zone for a hybrid distributed generation system. It is based on the computation of frequency spectrum variations over time using short-term Fourier transform and convolutional neural networks. For various islanding and non-islanding occurrences, the three-phase voltage at the point of common coupling is monitored, and time-series data is collected. Then computations for a set of multiple frequencies on scaled time-series data are carried out, and complex numbers are split into magnitude and phase values. To detect islanding and non-islanding occurrences, a modified convolutional neural network with forward propagation was utilized. For the IEC 61850-7-420 test system, several islanding and non-islanding scenarios are created and deployed to train the convolutional neural network for the proposed approach. The efficacy of the proposed islanding detection learning model is assessed using 5-fold cross-validation. The findings reveal that under normal and noisy conditions, the proposed methodology has zero non-detection zone with original dataset, excellent accuracy, selectivity, and sensitivity.

INDEX TERMS Convolution neural networks (CNN), distributed generation (DG), islanding detection, non-detection zone (NDZ), short-term-Fourier-transform (STFT).

I. INTRODUCTION

The quick integration of distributed generation (DG) has attracted increasing attention, because of energy market liberalization, capital investment, the need for stable and higher power quality (PQ), and environmental concerns. Electricity generation is centralized in a traditional electrical power system (EPS), and it is transferred to users via transmission and distribution networks. DG integration, apart from its paybacks and leads, also introduced new challenges and glitches in the power system such as unintentional islanding caused by unintentional tripping of the circuit breaker (CB) from the main utility. The critical issues related to unintentional islanding are personnel safety, overvoltage, reconnection out of phase, PQ, and equipment protection [1], [2], [3]. Islanding detection criteria and standards are provided in a variety of international and local standards. According to the international standards, islanding should be identified between 0.16 to 2 seconds [4], [5], [6], [7]. Therefore, the unintentional islanding detection problem has received much interest from researchers over the last decade to conquer this foremost concern of DG power systems. As a result, an accurate, dependable, and rapid islanding detection technique (IDT) is essential for the DG power system's security.

Research is ongoing, and several IDT have been described in the literature, with three basic categories: local, remote, and

The associate editor coordinating the review of this manuscript and approving it for publication was Ali Raza.

intelligent techniques. Active, passive, and hybrid islanding detection techniques are the three types of local techniques. Active methods like Slip-mode frequency shift (SMFS), Slip-mode voltage shift (SVS), Sandia frequency shift (SFS), etc. have noise and power quality issues [8], [9], [10], while passive islanding schemes like under/over voltage and frequency, voltage phase jump, harmonic measurement, etc. have a large non-detection zone (NDZ) and low speed [11], [12], [13]. Hybrid schemes are a combination of active and passive methods; they have a long detection time and complicated execution [14], [15]. Remote techniques need a contact link, and they are consistent for big systems, but for small scale and microgrid system remote techniques are impractical due to their complexity and high cost [16], [17].

Intelligent islanding detection schemes are considered the most desirable as they are faster and more reliable than local and remote schemes. The main reasons for this dominancy are fast detection, low NDZ, high accuracy, and negligible effect on PQ of the DG power system [18]. In [19] authors presented a hybrid IDT for multiple inverter-based DG that combines DT and SFS. In [20], a unique method based on active and reactive power for creating DT logic for the categorization of islanding and non-islanding occurrences was presented, that promptly correlates to NDZ. In [21], IDT was presented for inverter-based DG using naive-Bayes classifier for event classification and rotational invariance approach for feature extraction at the point of common coupling (PCC) to approximate the signal parameter.

A universal islanding detection solution for multi DGs was proposed using ANN in [22]. Using SVM, [23] introduced a novel IDT for single-phase inverter-based DG. phase inverter-based DG. IDT for hybrid DG with IEEE 30-bus proposed in [24] based on the SVM classifier. In [25], the authors introduced a unique hybrid approach for NDZ removal employing SFS and FL. In [26] author suggested an islanding detection system that uses fuzzy positive feedback (PF) to limit interfering injection. An IDT for inverter-based DG based on ANFIS has been presented in [27]. A novel ANFIS system methodology for detecting islanding in low-voltage inverter-interfaced microgrids was suggested in [28]. Deep neural learning was initially used and described in [29] to identify islanding and other grid disruptions in PV single-phase power production systems. In 2019, CNN was first used for PV DG power system applications, and IDT was proposed based on CNN image categorization [30].

This work's fundamental motivation is the in-depth literature review and investigation mentioned above. Intelligent IDT must have minimum NDZ, high precision, and quick detection times, as well as both inverter and synchronous based DG. This method eliminates the drawbacks of remote techniques, which require a communication link, work well for bigger systems, but are impractical because of their complexity and high cost [17]. Furthermore, this IDT resolves the issues with power quality, a big NDZ, and a lengthy detection time associated with local schemes [2]. The contribution of the study is outlined based on this research gap in the existing studies.

- This paper proposes a novel hybrid IDT that is a combination of CNN and short-term Fourier transform (STFT) spectrogram, with time-frequency domain analysis using time variations in the frequency spectrum is conducted for islanding detection of the DG-EPS.
- For islanding detection of DG-EPS, a modified convolutional neural network architecture is proposed, as CNN-based IDT does not require any threshold adjustments and communication link for detection.
- Extensive simulations are conducted for islanding that includes small and large power mismatch, while for non-islanding scenario; various line faults, load switching, and capacitor switching are considered. Additionally, the suggested IDT performs superbly in noise conditions with SNRs of 30, 35, and 40.
- Finally, the suggested scheme's performance is assessed using several indexes like accuracy, selectivity, sensitivity, NDZ, and noisy conditions. K-fold cross-validation method is adopted for better depiction of proposed algorithm performance, and reproducibility of the reported results.
- To illustrate the efficacy of the suggested method, it is also compared to existing state-of-the-art islanding techniques in term of accuracy, NDZ, multi DG, zero-power mismatch, non-islanding disturbances, and power quality.

To address the paper's goal, the remaining sections are organized as follows: In Section II Theoretical details of the STFT spectrogram and CNN are introduced. The proposed methodology and flow chart are explained in section III. Section IV represents the introduction of the test system, data mining, simulation results and extensive comparison. Lastly, in Section V, the conclusions proposed study is presented.

II. THEORETICAL DETAILS

A. STFT SPECTROGRAM

Signal and system techniques can retrieve the unseen/hidden attributes of the measured signal that are useful for islanding detection. Signal processing techniques such as STFT, wavelet transform (WT), S-transform (ST), hyperbolic S-transform (HST), and time-time transform (TTT) [24], [31], [32], [33], [34] are considered to enhance the operation of islanding detection especially for NDZ in passive techniques. The most popular method in frequency domain analysis is the Fourier transformation. It basically simulates a signal by computing sinusoidal terms at various frequencies. While the properties of the stationary signal at different frequencies are extracted, the temporal distribution of the different frequencies is not revealed. It, therefore, cannot address any momentary details relevant to fluctuations [35].

Therefore, STFT is used in this research for time-frequency analysis, STFT spectrogram is used to extract the voltage data on various islanding and non-islanding disturbances, and

then the mined numeric data is fed to CNN for classification of islanding and non-islanding. STFT is a Fourier transform modification that separates a signal into tiny frames, each of which may be stationary. The moving window evaluates these multiple frames of the signal. This moving window displays the link between time and frequency shift [32], [36]. Using the fast Fourier transform (FFT) to create a spectrogram is a digital procedure. In the temporal domain, discretely sampled data is divided into eight non-overlapping 360-sample chunks and Fourier transformed to generate the complex frequency spectra for each chunk. Later, the phase and magnitude of these frequency spectra are determined; this produces a vertical line in the image that represents a measurement of signal strength versus frequency for a certain period. These spectra can be ''laid side by side'' to produce the image or a three-dimensional surface [4], where power spectral density is represented by a color bar, to visually represent the obtained frequency spectra as shown in Fig. 1. STFT is essentially discrete Fourier transform (DFT) computations over short overlapping or non-overlapping windows, which for a discrete-time signal x(n) might be expressed as equation (1).

$$X(m,\omega) = \sum_{n=-\infty}^{\infty} x[n]\,\omega[n-m]e^{-j\omega n} \tag{1}$$

Where x[n] is the input signal to be transformed and w[n] is the window function. The squared magnitude of STFT results in a spectrogram representing the power spectral density of the function. According to the uncertainty principle, the time-frequency resolution of the resulting spectrum is determined by the window size used. A bigger size yields higher spectral, but lower temporal, resolution, whereas a smaller size yields the opposite.

B. CNN

The CNN is a well-known deep learning architecture influenced by the automatic visual experience of living beings. Over the last decade, the CNN has had groundbreaking results in a variety of pattern recognition-related fields, from image processing to voice recognition. The most advantageous function of CNNs is the reduction of the number of parameters in the ANN. The selection of features in supervised learning methods is a key stage in the training, testing, and deployment processes. Such attributes must be chosen correctly to ensure reasonable classification accuracy. CNNs, in contrast, use end-to-end learning, which means that the classifier discovers all the features and then classifies the images, resulting in a data-driven method [37]. A typical CNN model is a combination of a few main layers. The convolutions layer constructs a feature map to predict class probabilities. The batch normalization (BN) layer standardizes the inputs to a layer to avoid internal covariate shift. After calculating a nonlinear function of the input, a rectified linear unit (ReLU), activates the specific neuron. Pooling layers decrease the amount of information by retaining the most relevant information created by the convolution layer. Fully connected (FC)

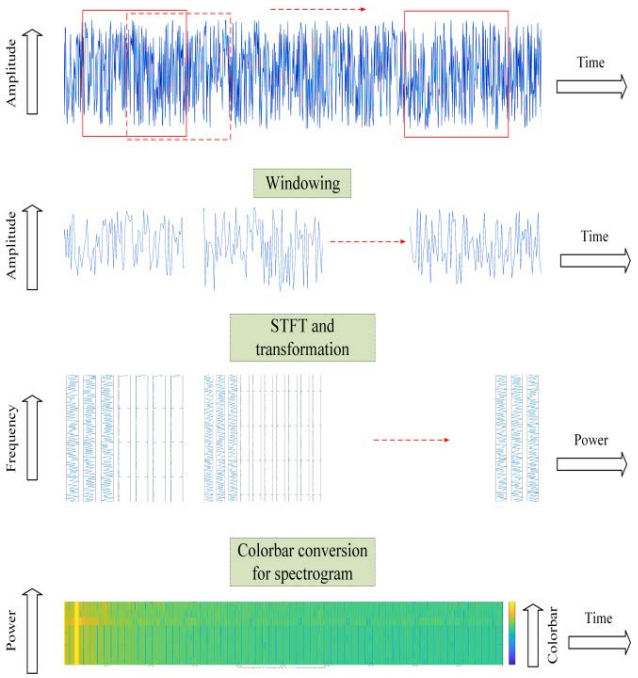

FIGURE 1. STFT working.

layers perform the following tasks: 1) the FC input layer can flatten output generated by the previous layer, 2) FC layers apply weights to simulate precise labels, and 3) the FC output layer produces final probabilities. Finally, the SoftMax layer measures the class likelihood for the input sample, which is mostly employed in combination with the cross-entropy (CE) loss function. Equation (2) is the mathematical description of five layers of CNN.

Convolution layer:

$$g_j^l = x_j^{l-1}(s,t) \times w_{ij}^l = \sum_{\sigma=-n1}^{n1}\sum_{\sigma=-n2}^{n2} x_j^{l-1}(s-\sigma, t-v) w_{ij}^l(\sigma, v) \tag{2a}$$

Activation or ReLU layer:

$$x_j^l = \max(0, \sum_{i\in Mj} g_j^l + b_j^l) \tag{2b}$$

Max Pooling (MP) layer:

$$x_j^{l+1} = f_p(b_j^{l+1}\left(x_j^l\right) + b_j^{l+1}) \tag{2c}$$

Fully connected (FC) layer:

$$x^{L-1} = f_c(\beta^{L-1}x^{L-2} + b^{L-1}) \tag{2d}$$

SoftMax layer:

$$z_d = \frac{e^{o_d}}{\sum_{c=1}^{C} e^{o_c}} \rightarrow \frac{e^{x_d^{L-1}}}{\sum_{c=1}^{C} e^{x_c^{L-1}}} \tag{2e}$$

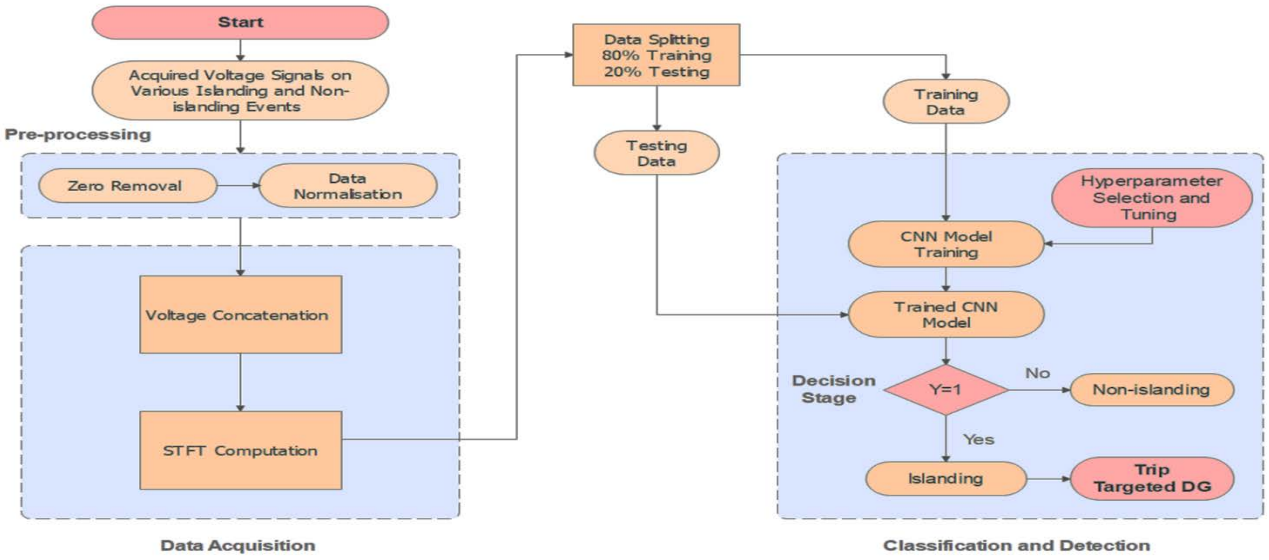

FIGURE 2. Flow chart of the proposed scheme.

The 'i' feature maps x_i^{l-1} of the preceding layer are convolved with the jth learnable filter (w_{ij}^l) appearing in the current or ith convolutional layer, which yields the jth new feature map (x_j^l) after employing activation or the ReLU function. This means that the current layer $l's$ new feature map is dependent on feature maps from the preceding layer l-1. The CNN calculates the divergence between the real distribution and the distribution created by the model using cross-entropy loss (Y) [38]. Y is computed using Equation (3)

$$Y\ (y, z) = -\sum_{d} y_d log(z_d) \tag{3}$$

III. PROPOSED ISLANDING DETECTION TECHNIQUE

In this section, proposed techniques and CNN architecture designs are discussed. The proposed IDT is based on CNN and STFT computation for time-frequency analysis; the stages of the proposed method are summarized as the flowchart in Fig. 2. The description and theory of both CNN and STFT are mentioned in section III. There are four phases of the anticipated IDT. At PCC, the three-phase voltage data is initially gathered under a variety of islanding and non-islanding conditions. In the second step, the three-phase voltage data are concatenated to create a single array of voltage data. The concatenated voltage data is then transformed into frequency spectrum time variations by STFT for time-frequency analysis in the 3rd stage. In the final stage, the phase and magnitude of the frequency spectrum numeric data concerning time variations are fed into the CNN for inherent feature learning and classification of islanding and non-islanding events.

For islanding detection, the developed CNN architecture is adapted for optimized training and test performance. The CNN architecture layers, convolution filter size, and training hyperparameters are chosen to acquire maximum accuracy and efficiency. The accuracy has direct link to the number of layers to a limit otherwise the CNN will start overfitting. In this case, three layers are selected for CNN islanding and non-islanding classification; the detailed architecture is presented in Table 1. After finalizing the architecture, the next important step is fine-tuning by varying various hyperparameters. Stochastic gradient descent with momentum (SGDM) optimizer is used in this architecture, and the best results and accuracy are captured with a learning rate (LR) of 0.0005. K-fold cross-validation is also implemented with k = 5 for this architecture.

During backpropagation in neural networks, the optimization algorithm SGDM estimates the gradient of error among current output of model and the desired output. It then backpropagates for updating the model weights, at the pace of given LR. The LR controls the amount of apportioned error that the weights of the model are updated with each time they are updated, such as at the end of each batch of training examples. While a very high LR may leads the model to diverge, lower LR can never get it to the optimal solution or to converge at slowly. Hence, the goal of the LR is to help the model converge quickly. In this work, we have empirically selected the hyperparameters through grid search, by LR staring with a broad range of high and low values and then narrowing the range down as per rate of model convergence.

IV. RESULTS AND DISCUSSIONS

A. SYSTEM UNDER STUDY

The suggested scheme is validated in the IEC 61850-7-420 DG power system. The test system consists of several DG units with both synchronous and inverter-based DG as shown in Fig. 3. The whole system was constructed in

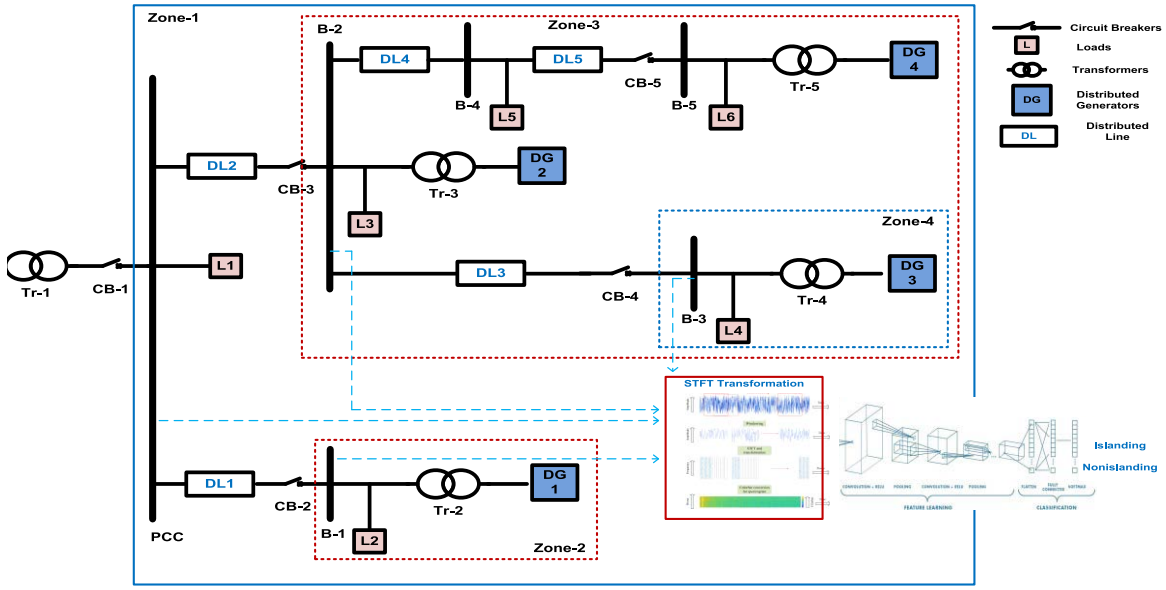

FIGURE 3. Test system for the proposed scheme.

TABLE 1. CNN architecture.

Type	Activations	Learnable Parameters
Input Layer	513*16*3	
Convolution Layer_1	513*16*8	Weights 2*2*3*8, Bias 1*1*8
BN Layer	513*16*8	Offset 1*1*8, Scale 1*1*8
ReLU Layer	513*16*8	
MP Layer	256*8*8	
Convolution Layer_2	256*8*16	Weights 2*2*8*16, Bias 1*1*16
BN Layer	256*8*16	Offset 1*1*16, Scale 1*1*16
ReLU Layer	256*8*16	
MP Layer	128*4*16	
Convolution Layer_3	128*4*32	Weights 2*2*16*32, Bias 1*1*32
BN Layer	128*4*32	Offset 1*1*32, Scale 1*1*32
ReLU Layer	128*4*32	
MP Layer	64*2*32	
FC Layer	1*1*10	Weights 10*4096, Bias 10*1
FC Layer	1*1*2	Weights 2*10, Bias 2*1
SoftMax Layer	1*1*2	
Classification Output Layer		

a (MATLAB/SIMULINK) environment, the complete details and parameters of test system illustrated in Tables 2 and 3 [39]. As shown in Fig. 1, the system is partitioned into four different zones for testing islanding events. Zone 1 contains all DGs and when CB1 is open the DG system goes into islanded mode. The zone 2 consists of synchronous based-DG only, while zone 3 has two inverter-based DGs and a synchronous DG. A zone 4 has inverter-based DG only and is islanded using CB4.

TABLE 2. DGs and transformer data for the test system.

DG	Power Rating	Voltage Rating
Synchronous based DGs (1 & 2)	4 MVA	2.4 kV
Inverter based DGs (3 & 4)	3 MVA	311 V
Transformer 1	20 MVA	120–25 kV
Transformer 2 & 3	5 MVA	2.4–25 kV
Transformer 4 & 5	5 MVA	0.311– 25 kV

TABLE 3. Load parameters for the test system.

Load	P (MW)	Q (MVAR)	Load	P (MW)	Q (MVAR)
L1	1.5	0.6	L4	1.5	0.6
L2	1.5	0.3	L5	0.5	0.1
L3	1.0	0.2	L6	1.0	0.3

B. DATA MINING FOR ISLANDING AND NON-ISLANDING SCENARIOS

Intelligent techniques are directly affected by the quality and quantity of data. To train the CNN we required a lot of training data for better generalization of learned features, so that it performs well for testing data. The data set preparation for CNN training involves STFT computation on scaled time series data of various islanding and non-islanding scenarios. The

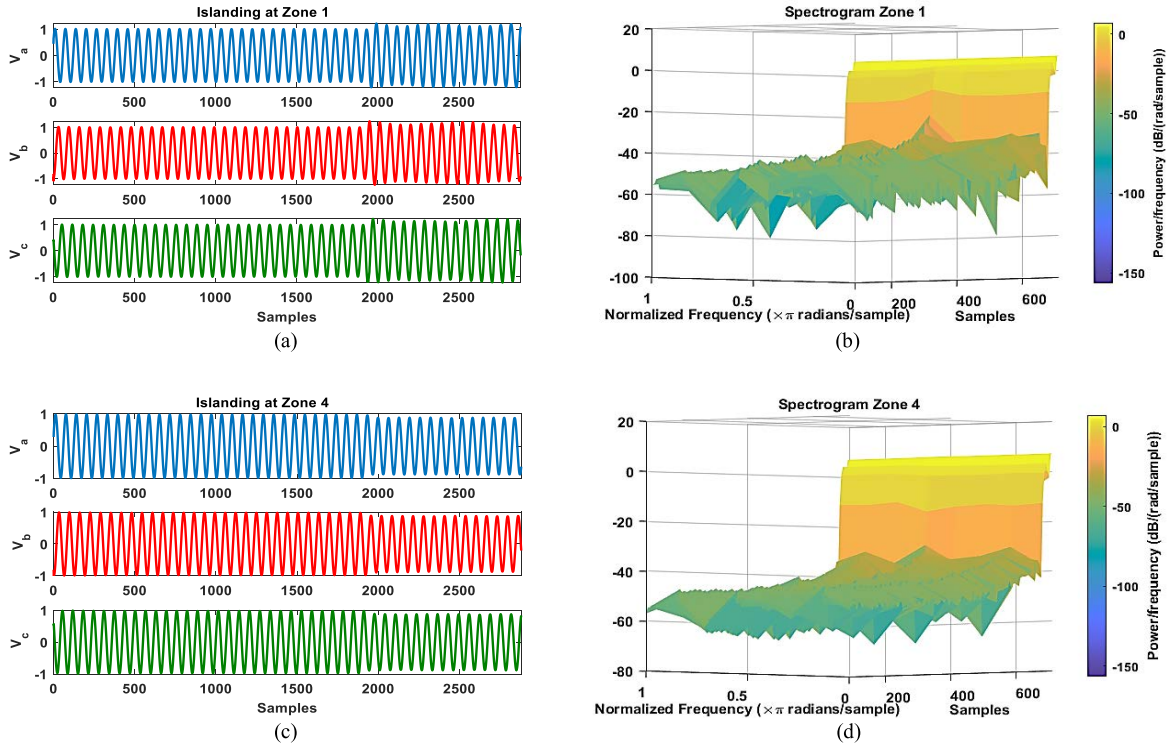

FIGURE 4. Behavior during islanding at zone 1 and 4: a) three phase voltage zone 1, b) spectrogram of zone 1, c) three phase voltage zone 4 and d) spectrogram of zone 4.

sampling frequency is kept at 3840 Hz and total simulation time is 0.75s. To test the proposed method, 3159 distinct cases were mined at PCC in the form of 3-phase voltage, 1785 cases for islanding, and 1374 cases for the non-islanding scenario. For islanding scenarios, the voltage data is extracted by varying the active power between 0 to ±50% and the reactive power in the range of 0 to ±25%. The most important situation during islanding is NDZ and in this case study 441 cases were considered within NDZ. The islanding cases are mined from all 4 zones of the test system. Similarly, for non-islanding the three different types of disturbances considered are all types of line faults at distribution lines 1 and 2. Single-line-to-ground (SLG), double-line-to-ground (DLG), double line (DL), and three phase to ground (TLG) are inserted for 0.1–100 Ω resistance. Load switching at L3 (0.3–3 MVA), L4 (30–500 kVA), and L5 (1–100 MVA). Finally, 90 cases of capacitor switching are considered to collect the voltage data at bus 3 (0.1–3 MVA), bus 4 (10–150 kVA), and bus 5 (1–10 MVA). Table 4 describes the complete details of islanding and non-islanding cases.

C. THE BEHAVIOR OF THE VOLTAGE SIGNAL DURING ISLANDING

Various islanding detection events are generated as summarized in Table 4. To validate the proposed algorithm's performance, all potential islanding instances are simulated. In addition, numerous active and reactive power imbalances between load and generation in the islanded network are examined for islanding identification. The bulk of current methodologies have trouble recognizing islanding when there is a little or tiny difference between the load and the power generation.

The islanding cases are produced at t = 0.5 s, by tripping different circuit breakers to formulate Zones 1, 2, 3, and 4. The voltage signal is monitored at PCC and the corresponding behaviors of the voltage signal are a form of STFT, and a spectrogram is captured. When there was almost no power difference between the DG generation and the load, the three-phase voltage did not display any notable changes. However, it exhibits a distinct characteristic in the time-frequency representation of the voltage signal throughout all islanding situations as shown in Fig. 4. The three phase voltage behavior for each islanding scenario at different zones are shown in (a) and (c) of each Fig, while (b) and (d) shows the corresponding spectrogram.

D. THE BEHAVIOR OF THE VOLTAGE SIGNAL DURING NON-ISLANDING

A reliable islanding detection approach should not malfunction in the presence of non-islanding disruptions. To demonstrate how the proposed IDT performs in non-islanding scenarios, a variety of short circuit failures, including some of the most common disturbances are used like load switching at various locations and capacitor switching at various busses

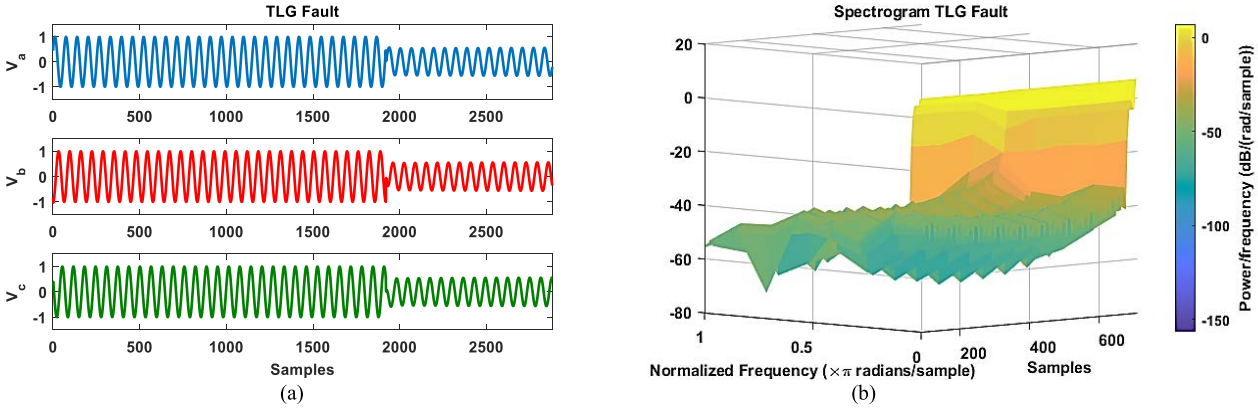

FIGURE 5. Behavior during non-islanding by TLG fault a) three phase voltage and b) spectrogram.

TABLE 4. Data mining for the proposed IDT.

Islanding and Non-islanding cases on various disturbances	No. of Cases
Islanding	**1785**
• Islanding by changing ΔP and ΔQ from (-50% to +50%) and (-25% to +25%) respectively.	1785
Non-islanding	**1374**
• Faults on bus 1 and bus 2 (SLG, DLG, and TLG) by changing fault resistance from (0.1–100 Ω)	1194
• Load switching on L3, L4, and L5 in the range of (0.3–30 MVA), (30–500 kVA), and (1–100 MVA) respectively.	90
• Capacitor switching on bus 3, bus 4, and bus 5 in the range of (0.1–30 MVA), (10-150 kVA), and (1–10 MVA) respectively.	90
Total islanding and non-islanding cases	**3159**

are explored. SLG, DLG, and TLG faults are examples of short-circuit faults.

1) SHORT CIRCUIT FAULTS

Short circuit faults are the most dangerous and difficult incidents to deal with in DG network. When a distribution network phase or phases are turned off, either directly or indirectly, several problems can occur. The existence of such defects in a distribution network might result in voltage and current variations, causing the islanding detection approach to malfunction. These differences, which are primarily SLG faults, cause misunderstanding between islanding and non-islanding occurrences. All three types (SLG, DLG and TLG) of line fault as detailed in Table 3 are injected into the examined test system after 0.5 seconds for this study as shown in Fig. 5. The three phase voltage behavior for TLG fault is presented in Fig. 5(a), while Fig. 5(b) displays the corresponding spectrogram.

2) LOAD SWITCHING

For the validation of islanding detection systems, load switching is also an essential element. Such an occurrence can result in significant voltage and current variations, which can lead to erroneous detection. This research looks at RLC load with active and reactive power changes as detailed in Table 3. The three phase voltage behavior for load switching at load 5 is displayed in Fig. 6(a), while Fig. 6(b) displays the corresponding spectrogram.

3) CAPACITOR SWITCHING

Finally, to accomplish capacitor switching, the capacitor bank is attached to the distributed test system. To simulate capacitor-switching occurrences, capacitor banks of varying ratings, as listed in Table 3, are linked to the DG power system. The three phase voltage behavior for load switching at bus 5 is shown in Fig. 7(a), while Fig. 7(b) shows the corresponding spectrogram.

E. NON-DETECTION ZONE ANALYSIS

An NDZ is often defined as a collection of active and reactive power imbalances in which voltage and frequency relays are unable to immediately identify an islanding event. Using (4) and (5), the NDZ boundary limits may be established, and the area with critical and non-critical operating conditions can be located [2].

$$\left(\frac{V}{V_{max}}\right)^2 - 1 \leq \frac{\Delta P}{P} \leq \left(\frac{V}{V_{min}}\right)^2 - 1 \tag{4}$$

$$Q_f\left((1-\left(\frac{f}{f_{min}}\right)^2\right) \leq \frac{\Delta Q}{P} \leq Q_f\left((1-\left(\frac{f}{f_{max}}\right)^2\right) \tag{5}$$

where V_{max}, V_{min}, f_{max}, and f_{min} are the maximum and minimum voltage/frequency. ΔP and ΔQ represent the active and reactive power mismatches while quality factor is represented using Q_f.

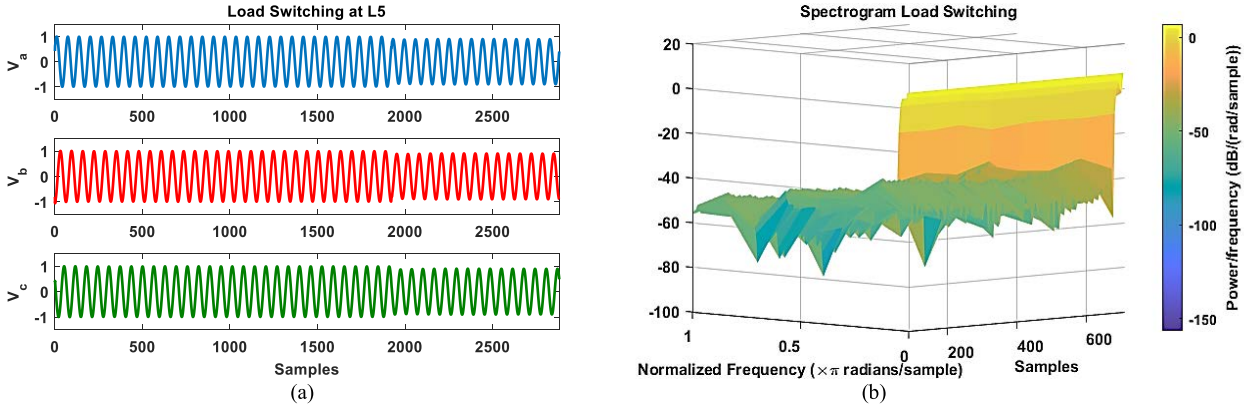

FIGURE 6. Behavior during non-islanding by load switching a) three phase voltage and b) spectrogram.

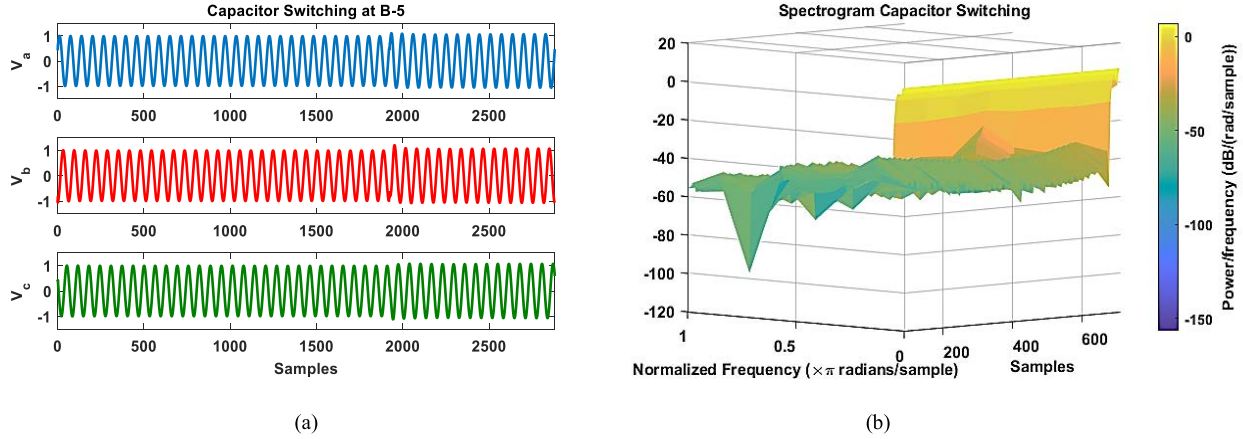

FIGURE 7. Behavior during non-islanding by capacitor switching a) three phase voltage and b) spectrogram.

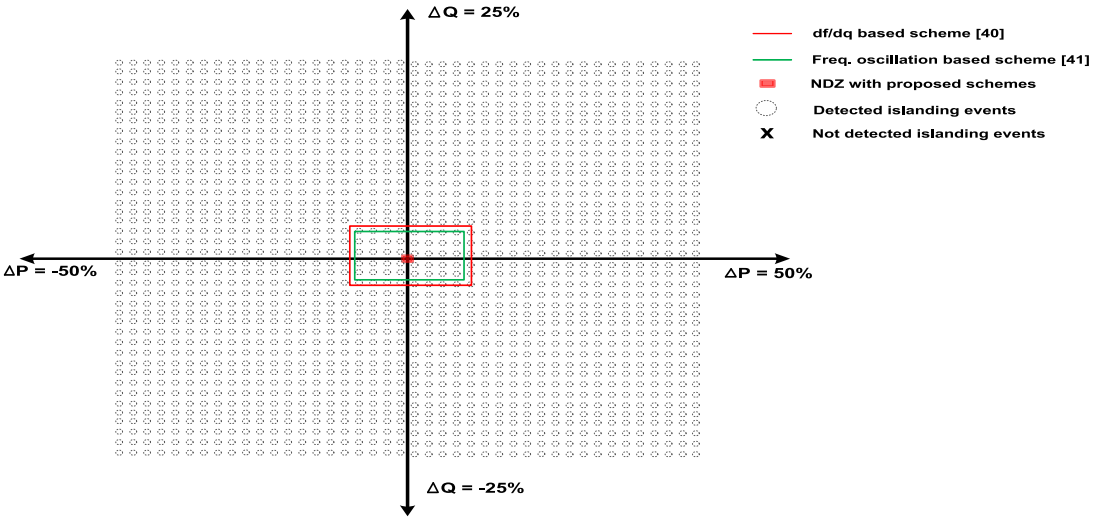

FIGURE 8. NDZ assessment of proposed IDT.

The NDZ index may also be used to assess the efficiency of any IDT. The NDZ is a zone where the difference between load and generation is 0% or approximately 0%. In the suggested system to estimate the NDZ, as all the cases of islanded

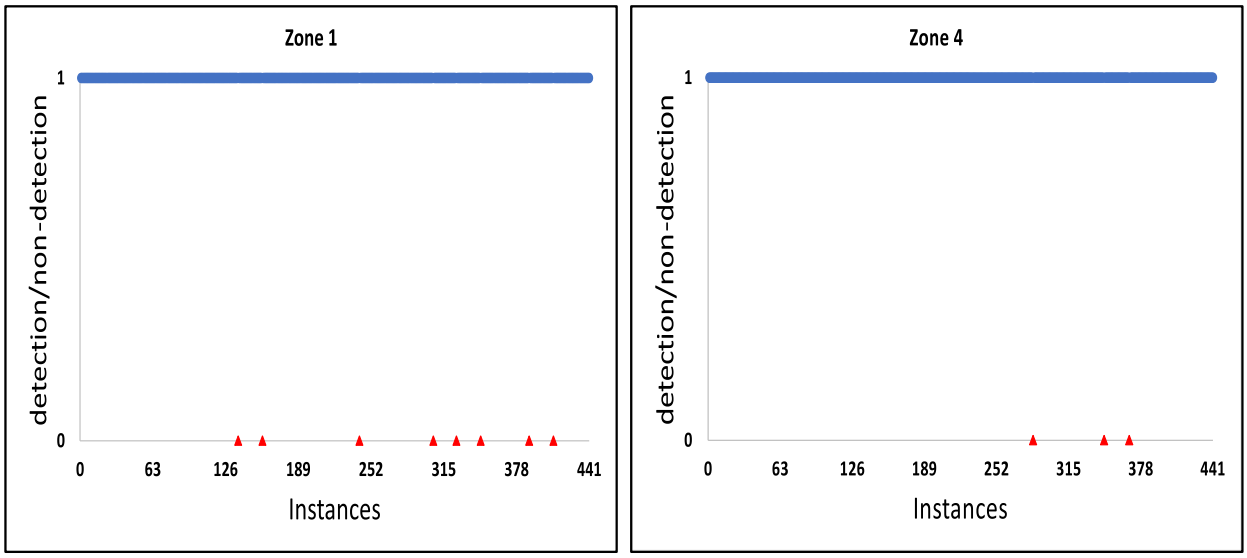

FIGURE 9. Misclassified instances of a) Zone 1 and b) Zone 4 with 40dB noise.

events with a (−50% to +50%) percent change in active and (−25% to +25%) percent reactive power were created. With original dataset the proposed scheme detects all the islanding cases accurately with zero NDZ as shown in Fig. 8. The NDZ of proposed method is compared with [40] and [41]. While with noisy data (40dB) only 8 instances were misclassified in Zone 1 out of 441 cases and only 3 cases were misclassified in Zone 4. Fig. 9(a)-(b) shows the misclassified instances of Zone 1 and Zone 4 with red triangle respectively.

F. RESULTS IN TERM OF PERFORMANCE INDICES

In this study, the data set is divided into training and test datasets with a proportion of 80% to 20%. The proposed IDT is validated using K-Fold validation. Extracted data is split into 5-folds. Training and testing data are separated, and the CNN is trained with 4-folds. The remaining 1-fold of data, which is entirely hidden for the CNN, is utilized for testing after CNN has been trained using 4-folds of the training data. There are situations in the data set with almost negligible power disparity, different faults, load switching, and capacitor switching. An intrinsic benefit of transforming the time-series data to STFT time-frequency data is that the variations in the frequency component of voltage variations are manifested in the pattern. The proposed IDT can properly distinguish islanding and non-islanding scenarios based on earlier unseen test data.

The proposed method was put to the test by including noise and uncertainty in both the training and testing data sets. A specific quantity of white Gaussian noise was added to the obtained dataset to distort it. Three levels of signal-to-noise ratio (SNR) were used in the simulations: 30, 35, and 40 dB. Noise is added to both training and test data, so that the technique's performance on noisy test data can be evaluated. The summarized confusion matrix with noisy data is shown in Table 5, the referred table provides a single result set for a sum of 4 variants (original + 40 dB + 35 dB + 30 dB data), while the detailed results in the form of performance indices like accuracy, sensitivity, and selectivity, and the confusion matrix for the study, are presented in Table 6. From the results of Table 5 and VI, it can be shown that the CNN performs well even with noisy conditions. With original data, the proposed scheme classifies islanding and non-islanding events with 100% accuracy. With 40 dB noise, the accuracy is 99.53%, and with 35 dB the average accuracy is 98.42% while with 30 dB noise the accuracy is 97.09% which is still reasonably good accuracy. Out of 7140 islanding cases, only 132 cases were misclassified in the collective dataset, while only 25 non-islanding cases were misclassified as islanding out of 5496 cases. The averaged accuracy with original and noisy data as shown in Table 5 is 98.76%. The accuracy of noisy data compared with the original data set is illustrated in Fig. 10. In Table 7, results from the suggested IDT are contrasted with those from other conventional and intelligent techniques.

TABLE 5. Summarized confusion matrix.

Total		Original Class		
		Islanding	Non-Islanding	
Predicted Class	Islanding	7008	132	98.15% (TNR)
	Non-Islanding	25	5471	99.55% (1/FNR)
		99.64% (TPR)	97.64% (1/FPR)	**98.76%**

V. DISCUSSION

Apart from the sights, integrating DGs into the electricity grid introduces a slew of additional issues. One of the

TABLE 6. Confusion matrix, accuracy over 5-folds, TPR, and TNR.

Data scheme	Confusion Matrix				Accuracy over 5-fold cross-validation							
	TP	FP	FN	TN	1st fold accuracy	2nd fold accuracy	3rd fold accuracy	4th fold accuracy	5th fold accuracy	Overall accuracy	TPR (sensitivity, recall)	TNR (specificity, selectivity)
Original data	1785	0	0	1374	100.00	100.00	100.00	100.00	100.00	**100.00%**	1.00	1.00
40dB noise	1774	11	4	1370	99.21	100.00	99.68	99.53	99.21	**99.53%**	1.00	0.99
35dB noise	1744	41	9	1365	98.10	98.73	98.10	98.42	98.73	**98.42%**	0.99	0.97
30dB noise	1705	80	12	1362	96.35	97.31	97.47	97.31	96.99	**97.09%**	0.99	0.94

TABLE 7. Comparison with other islanding techniques.

	Accuracy	NDZ	Multi DG	Zero power mismatch	Non-islanding Disturbances	Power Quality Maintained
[43]	92.86 %	Large	Yes	No	Yes	Yes
[42]	96.19 %	Zero	Yes	No	Yes	Yes
[43]	97.1 %	Small	No	No	Yes	Yes
[44]	-	Small	No	Yes	No	Yes
[45]	-	-	Yes	Yes	Yes	No
[46]	97.5 %	-	No	Yes	No	No
[29]	98.3 %	-	No	No	Yes	Yes
Proposed IDT	**98.76 %**	**Zero**	**Yes**	**Yes**	**Yes**	**Yes**

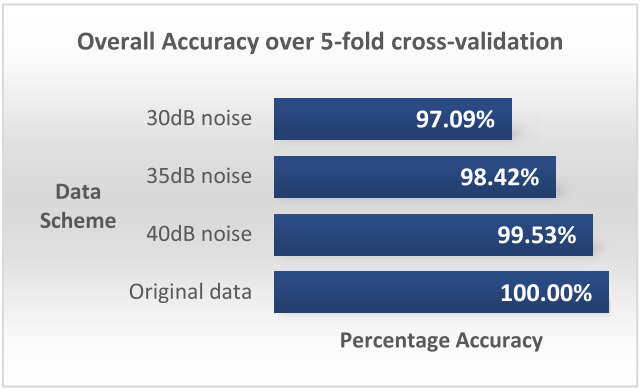

FIGURE 10. Overall accuracy comparison with original data and noisy data.

most challenging and essential issues is detecting islanding quickly. Malfunction to identify islanding during DG disconnection has a negative impact on system operations and local equipment, as well as putting utility workers in danger. This research suggested and evaluated an intelligent hybrid islanding detection technique on various islanding and non-islanding circumstances. The proposed methodology yields precise and dependable results. The proposed IDT uses just voltage signals; this technique may be utilized to identify and classify other power system disturbances. The proposed approach was tested on an Intel®Core (TM) i5-4690 CPU running at 3.50 GHz with 16 GB of RAM. The model was trained on a single NVIDIA GTX-1080 GPU with compute capability of 6.1, with MATLAB version 2021a.

VI. CONCLUSION

Using a novel hybrid IDT, this work presented a classification of islanding and non-islanding occurrences for hybrid DG test systems with both inverter-based and synchronous-based machines. STFT is used to transform time-series data recorded at PCC into a spectrum of frequencies with temporal variations in this research. These are grouped in phase and magnitude to train the constructed CNN for the classification of islanding and non-islanding scenarios. Under these conditions, a total of 3159 unique cases are gathered. The proposed IDT's performance is verified using 5-fold validation, and the CNN is also trained on noisy data with 40, 35, and 30 dB noise levels where most of the passive relays fail. 100% accuracy is achieved with the original dataset with zero NDZ, while an average accuracy of 98.76% is achieved applying the proposed IDT with the noisy dataset. Also, the proposed IDT has the fast detection time, which is very critical consideration in selecting islanding detection technique. The results reflect that frequency domain features contribute significantly to the CNN's performance for islanding detection, and these features need to be localized in time. The findings also imply that efficient DG islanding detection in real-time applications may be accomplished using deep learning-based approaches. The authors are going to implement the practical system of our proposed scheme in future work.

REFERENCES

[1] A. Khamis, H. Shareef, E. Bizkevelci, and T. Khatib, "A review of islanding detection techniques for renewable distributed generation systems," *Renew. Sustain. Energy Rev.*, vol. 28, pp. 483–493, Dec. 2013, doi: 10.1016/j.rser.2013.08.025.

[2] A. Hussain, C.-H. Kim, and A. Mehdi, "A comprehensive review of intelligent islanding schemes and feature selection techniques for distributed generation system," *IEEE Access*, vol. 9, pp. 146603–146624, 2021.
[3] C. Li, C. Cao, Y. Cao, Y. Kuang, L. Zeng, and B. Fang, "A review of islanding detection methods for microgrid," *Renew. Sustain. Energy Rev.*, vol. 35, pp. 211–220, Jul. 2014, doi: 10.1016/j.rser.2014.04.026.
[4] T. Basso, "IEEE 1547 and 2030 standards for distributed energy resources interconnection and interoperability with the electricity grid," Nat. Renew. Energy Lab. (NREL), Golden, CO, USA, Tech. Rep. NREL/TP-5D00-63157, 2014, doi: 10.2172/1166677.
[5] R. M. Hudson, T. Thorne, F. Mekanik, M. R. Behnke, S. Gonzalez, and J. Ginn, "Implementation and testing of anti-islanding algorithms for IEEE 929-2000 compliance of single phase photovoltaic inverters," in *Proc. 29th IEEE Photovolt. Spec. Conf.* IEEE, May 2002, pp. 1414–1419, doi: 10.1109/PVSC.2002.1190874.
[6] H. Karimi, A. Yazdani, and R. Iravani, "Negative-sequence current injection for fast islanding detection of a distributed resource unit," *IEEE Trans. Power Electron.*, vol. 23, no. 1, pp. 298–307, Jan. 2008, doi: 10.1109/TPEL.2007.911774.
[7] H. H. Figueira, H. L. Hey, L. Schuch, C. Rech, and L. Michels, "Brazilian grid-connected photovoltaic inverters standards: A comparison with IEC and IEEE," in *Proc. IEEE 24th Int. Symp. Ind. Electron. (ISIE)*, Jun. 2015, pp. 1104–1109, doi: 10.1109/ISIE.2015.7281626.
[8] R. Haider, C. H. Kim, T. Ghanbari, S. B. A. Bukhari, M. Saeed uz Zaman, S. Baloch, and Y. S. Oh, "Passive islanding detection scheme based on autocorrelation function of modal current envelope for photovoltaic units," *IET Gener., Transmiss. Distrib.*, vol. 12, no. 3, pp. 726–736, Feb. 2018, doi: 10.1049/iet-gtd.2017.0823.
[9] H. H. Zeineldin, E. F. El-Saadany, and M. M. A. Salama, "Impact of DG interface control on islanding detection and nondetection zones," *IEEE Trans. Power Del.*, vol. 21, no. 3, pp. 1515–1523, Jul. 2006, doi: 10.1109/TPWRD.2005.858773.
[10] S. K. G. Manikonda and D. N. Gaonkar, "Comprehensive review of IDMs in DG systems," *IET Smart Grid*, vol. 2, no. 1, pp. 11–24, Mar. 2019, doi: 10.1049/iet-stg.2018.0096.
[11] S. D. Kermany, M. Joorabian, S. Deilami, and M. A. S. Masoum, "Hybrid islanding detection in microgrid with multiple connection points to smart grids using fuzzy-neural network," *IEEE Trans. Power Syst.*, vol. 32, no. 4, pp. 2640–2651, Jul. 2017, doi: 10.1109/TPWRS.2016.2617344.
[12] J.-S. Kim, C.-H. Kim, Y.-S. Oh, G.-J. Cho, and J.-S. Song, "An islanding detection method for multi-RES systems using the graph search method," *IEEE Trans. Sustain. Energy*, vol. 11, no. 4, pp. 2722–2731, Oct. 2020, doi: 10.1109/TSTE.2020.2972948.
[13] S. Admasie, S. B. A. Bukhari, R. Haider, T. Gush, and C.-H. Kim, "A passive islanding detection scheme using variational mode decomposition-based mode singular entropy for integrated microgrids," *Electr. Power Syst. Res.*, vol. 177, Dec. 2019, Art. no. 105983, doi: 10.1016/j.epsr.2019.105983.
[14] H. H. Zeineldin and S. Kennedy, "Sandia frequency-shift parameter selection to eliminate nondetection zones," *IEEE Trans. Power Del.*, vol. 24, no. 1, pp. 486–487, Jan. 2009, doi: 10.1109/TPWRD.2008.2005362.
[15] P. Nayak, R. K. Mallick, and S. Dhar, "Novel hybrid signal processing approach based on empirical mode decomposition and multiscale mathematical morphology for islanding detection in distributed generation system," *IET Gener., Transmiss. Distrib.*, vol. 14, no. 26, pp. 6715–6725, Dec. 2020, doi: 10.1049/iet-gtd.2020.0780.
[16] G. Bayrak and E. Kabalci, "Implementation of a new remote islanding detection method for wind–solar hybrid power plants," *Renew. Sustain. Energy Rev.*, vol. 58, pp. 1–15, May 2016, doi: 10.1016/j.rser.2015.12.227.
[17] J. Merino, P. Mendoza-Araya, G. Venkataramanan, and M. Baysal, "Islanding detection in microgrids using harmonic signatures," *IEEE Trans. Power Del.*, vol. 30, no. 5, pp. 2102–2109, Oct. 2015, doi: 10.1109/TPWRD.2014.2383412.
[18] A. Hussain, C. H. Kim, and S. Admasie, "An intelligent islanding detection of distribution networks with synchronous machine DG using ensemble learning and canonical methods," *IET Gener. Transm. Distrib.*, vol. 15, pp. 1–14, Jun. 2021, doi: 10.1049/gtd2.12256.
[19] R. Azim, F. Li, Y. Xue, M. Starke, and H. Wang, "An islanding detection methodology combining decision trees and Sandia frequency shift for inverter-based distributed generations," *IET Gener., Transmiss. Distrib.*, vol. 11, no. 16, pp. 4104–4113, Nov. 2017, doi: 10.1049/iet-gtd.2016.1617.
[20] Q. Cui, K. El-Arroudi, and G. Joós, "Islanding detection of hybrid distributed generation under reduced non-detection zone," *IEEE Trans. Smart Grid*, vol. 9, no. 5, pp. 5027–5037, Sep. 2018, doi: 10.1109/TSG.2017.2679101.
[21] W. K. A. Najy, H. H. Zeineldin, A. H. K. Alaboudy, and W. L. Woon, "A Bayesian passive islanding detection method for inverter-based distributed generation using ESPRIT," *IEEE Trans. Power Del.*, vol. 26, no. 4, pp. 2687–2696, Oct. 2011, doi: 10.1109/TPWRD.2011.2159403.
[22] O. N. Faqhruldin, E. F. El-Saadany, and H. H. Zeineldin, "A universal islanding detection technique for distributed generation using pattern recognition," *IEEE Trans. Smart Grid*, vol. 5, no. 4, pp. 1985–1992, Jul. 2014, doi: 10.1109/TSG.2014.2302439.
[23] B. Matic-cuka and M. Kezunovic, "Islanding detection for inverter-based distributed generation using support vector machine method," *IEEE Trans. Smart Grid*, vol. 5, no. 6, pp. 2676–2686, Nov. 2014, doi: 10.1109/TSG.2014.2338736.
[24] S. R. Mohanty, N. Kishor, P. K. Ray, and J. P. S. Catalo, "Comparative study of advanced signal processing techniques for islanding detection in a hybrid distributed generation system," *IEEE Trans. Sustain. Energy*, vol. 6, no. 1, pp. 122–131, Jan. 2015, doi: 10.1109/TSTE.2014.2362797.
[25] H. Vahedi and M. Karrari, "Adaptive fuzzy Sandia frequency-shift method for islanding protection of inverter-based distributed generation," *IEEE Trans. Power Del.*, vol. 28, no. 1, pp. 84–92, Jan. 2013, doi: 10.1109/TPWRD.2012.2219628.
[26] C. R. Aguiar, G. Fuzato, R. F. Bastos, A. F. Q. Gonçalves, and R. Q. Machado, "Hybrid fuzzy anti-islanding for grid-connected and islanding operation in distributed generation systems," *IET Power Electron.*, vol. 9, no. 3, pp. 512–518, Mar. 2016, doi: 10.1049/iet-pel.2014.0717.
[27] F. Hashemi, N. Ghadimi, and B. Sobhani, "Islanding detection for inverter-based DG coupled with using an adaptive neuro-fuzzy inference system," *Int. J. Electr. Power Energy Syst.*, vol. 45, no. 1, pp. 443–455, Feb. 2013, doi: 10.1016/j.ijepes.2012.09.008.
[28] D. Mlakic, H. R. Baghaee, and S. Nikolovski, "A novel ANFIS-based islanding detection for inverter-interfaced microgrids," *IEEE Trans. Smart Grid*, vol. 10, no. 4, pp. 4411–4424, Jul. 2019, doi: 10.1109/TSG.2018.2859360.
[29] X. Kong, X. Xu, Z. Yan, S. Chen, H. Yang, and D. Han, "Deep learning hybrid method for islanding detection in distributed generation," *Appl. Energy*, vol. 210, pp. 776–785, Jan. 2018, doi: 10.1016/j.apenergy.2017.08.014.
[30] S. K. G. Manikonda and D. N. Gaonkar, "IDM based on image classification with CNN," *J. Eng.*, vol. 2019, no. 10, pp. 7256–7262, Oct. 2019, doi: 10.1049/joe.2019.0025.
[31] C.-T. Hsieh, J.-M. Lin, and S.-J. Huang, "Enhancement of islanding-detection of distributed generation systems via wavelet transform-based approaches," *Int. J. Electr. Power Energy Syst.*, vol. 30, no. 10, pp. 575–580, Dec. 2008, doi: 10.1016/j.ijepes.2008.08.006.
[32] S. Raza, H. Mokhlis, H. Arof, J. A. Laghari, and L. Wang, "Application of signal processing techniques for islanding detection of distributed generation in distribution network: A review," *Energy Convers. Manage.*, vol. 96, pp. 613–624, May 2015, doi: 10.1016/j.enconman.2015.03.029.
[33] M. Hanif, M. Basu, and K. Gaughan, "Development of EN50438 compliant wavelet-based islanding detection technique for three-phase static distributed generation systems," *IET Renew. Power Gener.*, vol. 6, no. 4, p. 289, 2012, doi: 10.1049/iet-rpg.2011.0290.
[34] P. K. Ray, S. R. Mohanty, and N. Kishor, "Disturbance detection in grid-connected distributed generation system using wavelet and S-transform," *Electr. Power Syst. Res.*, vol. 81, no. 3, pp. 805–819, Mar. 2011, doi: 10.1016/j.epsr.2010.11.011.
[35] M. Karimi, H. Mokhtari, and M. R. Iravani, "Wavelet based on-line disturbance detection for power quality applications," in *Proc. IEEE Power Eng. Soc. Transm. Distrib. Conf.*, vol. 1, Oct. 2001, p. 175.
[36] P. K. Dash, B. K. Panigrahi, D. K. Sahoo, and G. Panda, "Power quality disturbance data compression, detection, and classification using integrated spline wavelet and S-transform," *IEEE Trans. Power Del.*, vol. 18, no. 2, pp. 595–600, Apr. 2003, doi: 10.1109/TPWRD.2002.803824.
[37] Y. Sun, B. Wang, J. Jin, and X. Wang, "Deep convolutional network method for automatic sleep stage classification based on neurophysiological signals," in *Proc. 11th Int. Congr. Image Signal Process., Biomed. Eng. Informat. (CISP-BMEI)*, Oct. 2018, pp. 1–5, doi: 10.1109/CISP-BMEI.2018.8633058.
[38] G. Hussain, M. K. Maheshwari, M. L. Memon, M. S. Jabbar, and K. Javed, "A CNN based automated activity and food recognition using wearable sensor for preventive healthcare," *Electronics*, vol. 8, no. 12, p. 1425, Nov. 2019, doi: 10.3390/electronics8121425.

[39] T. Chakravorti, R. K. Patnaik, and P. K. Dash, "Detection and classification of islanding and power quality disturbances in microgrid using hybrid signal processing and data mining techniques," *IET Signal Process.*, vol. 12, no. 1, pp. 82–94, Feb. 2018, doi: 10.1049/iet-spr.2016.0352.
[40] S. Raza, H. Mokhlis, H. Arof, J. A. Laghari, and H. Mohamad, "A sensitivity analysis of different power system parameters on islanding detection," *IEEE Trans. Sustain. Energy*, vol. 7, no. 2, pp. 461–470, Apr. 2016, doi: 10.1109/TSTE.2015.2499781.
[41] G. Marchesan, M. R. Muraro, G. Cardoso, L. Mariotto, and A. P. de Morais, "Passive method for distributed-generation island detection based on oscillation frequency," *IEEE Trans. Power Del.*, vol. 31, no. 1, pp. 138–146, Feb. 2016, doi: 10.1109/TPWRD.2015.2438251.
[42] N. W. A. Lidula and A. D. Rajapakse, "A pattern-recognition approach for detecting power islands using transient signals—Part II: Performance evaluation," *IEEE Trans. Power Del.*, vol. 27, no. 3, pp. 1071–1080, Jul. 2012, doi: 10.1109/TPWRD.2012.2187344.
[43] D. Kumar and P. S. Bhowmik, "Artificial neural network and phasor data-based islanding detection in smart grid," *IET Gener., Transmiss. Distrib.*, vol. 12, no. 21, pp. 5843–5850, Nov. 2018, doi: 10.1049/iet-gtd.2018.6299.
[44] V. Kleftakis, D. Lagos, C. Papadimitriou, and N. D. Hatziargyriou, "Seamless transition between interconnected and islanded operation of DC microgrids," *IEEE Trans. Smart Grid*, vol. 10, no. 1, pp. 248–256, Jan. 2019, doi: 10.1109/TSG.2017.2737595.
[45] A. M. I. Mohamad and Y. A.-R.-I. Mohamed, "Assessment and performance comparison of positive feedback islanding detection methods in DC distribution systems," *IEEE Trans. Power Electron.*, vol. 32, no. 8, pp. 6577–6594, Aug. 2017, doi: 10.1109/TPEL.2016.2618220.
[46] G. S. Seo, K. C. Lee, and B. H. Cho, "A new DC anti-islanding technique of electrolytic capacitor-less photovoltaic interface in DC distribution systems," *IEEE Trans. Power Electron.*, vol. 28, no. 4, pp. 1632–1641, Apr. 2013, doi: 10.1109/TPEL.2012.2208226.

ARIF HUSSAIN (Member, IEEE) received the B.S. degree in electrical engineering, in 2014, and the M.S. degree in electrical (power) engineering from the National University of Science and Technology (NUST), Pakistan, in 2019. He is currently pursuing the Ph.D. degree with the Electrical and Electronics Department, Sungkyunkwan University (SKKU), South Korea. His doctoral research interests include employ and develop modern machine and deep learning techniques for renewable energy forecasting, islanding detection, and power system protection in hybrid AC/DC microgrids systems.

CHUL-HWAN KIM (Fellow, IEEE) received the B.S., M.S., and Ph.D. degrees in electrical engineering from Sungkyunkwan University, Suwon, South Korea, in 1982, 1984, and 1990, respectively. In 1990, he joined Jeju National University, Jeju, South Korea, as a Full-Time Lecturer. He was a Visiting Academic at the University of Bath, Bath, U.K., in 1996, 1998, and 1999. He has been a Professor with the College of Information and Communication Engineering, Sungkyunkwan University, since 1992, where he is currently the Director of the Center for Power Information Technology. His current research interests include power system protection, artificial intelligence applications for protection and control, modeling, and protection of microgrids and DC systems.

MUHAMMAD SHAHID JABBAR received the B.E. degree in electronics engineering from the Dawood University of Engineering and Technology, Pakistan, in 2013, and the M.S. and Ph.D. degrees in computer engineering from Sungkyunkwan University (SKKU), Suwon, South Korea, in 2022. His doctoral research was to employ and develop modern deep learning techniques using multi-modal vision and textual data for convergence applications involving multi-sensory interaction and cross-modular associations. During his Ph.D., he was a Researcher at the Media System Laboratory (MSL) and the Human ICT Laboratory (H-Lab) at SKKU. He worked as an Engineer Operations for Multimedia and Broadband at Pakistan Telecommunication Company Ltd. His current research interests include medical image processing, sequence data analysis, and multimodal deep learning applications.